PHYSICAL REVIEW D VOLUME 48, NUMBER 3 1 AUGUST 1993

Structure function formulation of $e^+e^- \to f\bar{f}$ around the Z^0 resonance in a realistic setup

Guido Montagna and Fulvio Piccinini
Dipartimento di Fisica Nucleare e Teorica, Università di Pavia, Istituto Nazionale di Fisica Nucleare, Sezione di Pavia, Via Bassi 6, 27100 Pavia, Italy

Oreste Nicrosini
Istituto Nazionale de Fisica Nucleare, Sezione di Pavia, Via Bassi 6, 27100 Pavia, Italy
(Received 9 March 1993)

A structure function approach to e^+e^- annihilation into fermion pairs and to large-angle Bhabha scattering at energies reached at the CERN LEP and/or SLAC SLC is described. Higher-order QED corrections to cross sections and forward-backward asymmetries are computed according to a semianalytical procedure which accounts for realistic experimental cuts on the final state fermions. The effect of cuts on the $f\bar{f}$ acollinearity angle, energies or invariant mass, and angular acceptance of the outgoing fermions is investigated at the level of initial state radiation. The interplay between initial- and final-state QED corrections in the presence of experimental cuts is also discussed. In the case of Bhabha scattering the contribution of unresolved hard collinear photons to calorimetric measurement is analytically included as well. A general formula for QED effects in the presence of realistic cuts is proposed and analytically worked out in order to obtain fast and high-precision numerical predictions.

PACS number(s): 13.10.+q, 13.40.Ks

I. INTRODUCTION

In a recent paper [1] a *realistic* theoretical approach to e^+e^- annihilation into fermion pairs and to large-angle Bhabha scattering around the Z^0 peak has been described. Reference [1] represents the completion of a rather ambitious program, started more or less one year ago and aimed at analyzing data from the CERN e^+e^- collider LEP through a direct comparison between experimental results for cross sections and asymmetries actually measured, i.e., on a realistic experimental setup, and the corresponding theoretical predictions within the minimal standard model (MSM). All the corrections, pure weak, QED, and QCD, necessary for such a realistic description, i.e., a description including energy or invariant-mass thresholds, cuts on the acollinearity angle, and angular acceptance of the outgoing fermions, have been included in the formulation [1]. Correspondingly, a semianalytical program (TOPAZ0) [2], designed for computing observables and fitting cross sections and forward-backward asymmetries at energies reached at LEP and/or the SLAC Linear Collider (SLC), has been developed and used to analyze LEP data and in particular to derive constraints on the unknown parameters (M_Z, m_t, m_H, and α_s) [1, 3] of the MSM of the electroweak and strong interactions.

The formulation and its interplay with the experimental results as described in [1] constitutes, as already stated, the achievement of a project aiming at an analysis of the MSM by directly comparing theoretical cross sections and asymmetries with the experimental ones without the need of relying upon the results for the Z^0 parameters (total and partial widths, peak cross sections, deconvoluted asymmetries, and so on) published by the LEP Collaborations. In order to succeed in this program, the formalism of the structure functions (SF's) [4, 5] for the evaluation of QED corrections and a complete one-loop calculation of pure weak corrections, together with leading higher-order terms [6, 7], were chosen as basilar ingredients of the formulation.

The interfacing of the various kinds of corrections required some preliminary steps. In Ref. [8] pure weak corrections were successfully interfaced with the SF formulation, previously given in [9], for QED corrections in the presence of cuts, by constructing an improved Born approximation essentially based on [6, 7]. The interplay between electroweak and strong corrections was studied in [10]. The accuracy of the obtained results was critically checked against independent calculations for typical realistic configurations.

These comparisons pointed out that the approximate description of the final-state radiation adopted in [9] was not appropriate in order to give theoretical predictions at the per mill level in particularly exclusive situations. Moreover, for the fitting purposes discussed above the QED formulation of [9] revealed to be not suitable from the point of view of CPU time requirements, showing the need of further analytical developments of the approach at the level of initial-state radiation.

The treatment of final-state QED corrections over a realistic experimental setup was improved by integrating the full matrix element of $e^+e^- \to f\bar{f}\gamma$ (with γ emitted by the final state) over the three-particle phase space allowed by cuts and deriving completely analytic formulas exact at $O(\alpha)$ [11]. As far as initial-state radiation in the presence of cuts is concerned, a proper strategy was

adopted in order to improve the SF formulation proposed in [9] and it has already been sketched in Ref. [1].

The aim of this paper is to give about the subject of QED corrections in realistic setup more details and formulas not reported in Ref. [1] and to describe in a self-consistent way the theoretical QED SF formulation developed in order to carry out the general program discussed in [1]. Pure weak and QCD corrections are not considered in this work, but their formulation can be found in [1], which the reader is referred to for details about non-QED effects, comparisons with independent formulations, overall numerical results, and analysis of LEP data.

Semianalytical and Monte Carlo approaches, based on different theoretical strategies, to realistic e^+e^- processes at LEP/SLC energies are already available in the literature and can be found in [8, 9, 12–17]. The cross-checks so far available [8, 14, 15], although showing a generally satisfactory agreement if compared with present day experimental errors, point out that, especially when considering Bhabha scattering, improvements and refinements on the subject of *realistic* QED corrections are possible and a better understanding of the theoretical uncertainties is mandatory.

The article is organized as follows. In Sec. II we briefly describe the kinematics of an e^+e^- collision with initial-state radiation within a soft and/or collinear approximation. In Sec. III we discuss the conditions imposed by realistic experimental cuts on the initial-state radiation phase space. The interplay between cuts and final-state radiation is tackled in Sec. IV, which summarizes analytic results derived in previous works [11, 18]. Section V contains the general description of the approach to the calculation of QED corrections to physical observables (cross section and forward-backward asymmetry) for pure s-channel annihilation both in inclusive and realistic configurations. Section VI is devoted to explaining some technical details adopted in the calculation of the corrected observables. Section VII describes the application of the procedure to large-angle Bhabha scattering, while in Sec. VIII we give our conclusions. Appendixes A and B contain some useful analytical formulas recalled in the text.

II. KINEMATICS

We describe the kinematics of the e^+e^- process in the laboratory frame [19], where, before initial-state electromagnetic radiation, the incoming electron and positron have the same energy E. Before colliding, the two particles can radiate photons and reduce their energy to x_1E and x_2E, respectively. As a consequence, the center of mass of the hard-scattering process is boosted with respect to the laboratory frame, and the scattering angles ϑ_1 and ϑ_2 as well as the energies E_1 and E_2 of the outgoing fermions are in general different (see Fig. 1). We will consider a soft and/or collinear radiation approximation, neglecting emission from the initial state of hard noncollinear photons which are strongly suppressed in presence of a resonance. By virtue of energy-momentum conservation the following conditions can be easily derived:

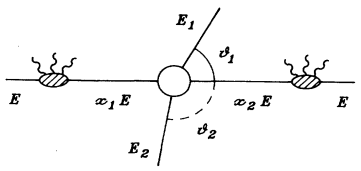

FIG. 1. Kinematics for a realistic e^+e^- collision in the laboratory frame. Because of initial-state radiation (external blobs on the beam line), the electron and positron reduce their energy to x_1E and x_2E. The central blob represents the hard-scattering process. The outgoing fermions emerge with different energies (E_1 and E_2) and angles (ϑ_1 and ϑ_2).

$$
\begin{aligned}
(x_1+x_2)E &= E_1+E_2,\\
E_1\sin\vartheta_1 &= E_2\sin\vartheta_2,\\
(x_1-x_2)E &= E_1\cos\vartheta_1+E_2\cos\vartheta_2.
\end{aligned}
$$

Choosing x_1, x_2, and the fermion-scattering angle ϑ_1 as independent variables, the previous equations can be solved analytically to get the final energies E_1 and E_2 and the cosine of the antifermion scattering angle ϑ_2. In the ultrarelativistic limit the solution reads

$$E_1=\frac{E}{2}\,\frac{x_p^2-x_m^2}{x_p-x_m\cos\vartheta_1}, \tag{2.1}$$

$$E_2=\frac{E}{2}\,\frac{x_p^2-2x_mx_p\cos\vartheta_1+x_m^2}{x_p-x_m\cos\vartheta_1}, \tag{2.2}$$

$$\cos\vartheta_2=\frac{x_mE-E_1\cos\vartheta_1}{E_2}, \tag{2.3}$$

where, for the sake of simplicity, we have introduced the notation $x_p=x_1+x_2$ and $x_m=x_1-x_2$. It is worth noting that knowledge of the analytical solutions of the kinematics is essential, as shown in the next section, to derive the portion of initial-state radiation phase space allowed by realistic experimental cuts.

III. REALISTIC CUTS ON THE INITIAL-STATE RADIATION PHASE SPACE

Usually, in a realistic experimental setup cuts on the the energies or invariant mass, acollinearity angle and angular acceptance of the outgoing fermions are imposed. As a consequence of Eqs. (2.1)–(2.3) each of these cuts introduces limits on the possible values for x_1 and x_2, which, in the case of a totally inclusive setup, would only be limited by the minimum invariant mass of the $f\bar{f}$ pair through the condition $x_1x_2\geq\frac{4m_f^2}{s}$.

Let us briefly examine the conditions imposed by each kind of cut.

Cuts on the scattering angles

Since we treat the fermion scattering angle ϑ_1 as an independent variable, we have to analyze the constraint on the phase space imposed by a cut on the antifermion-scattering angle ϑ_2. Limiting our analysis to symmet-

ric angular cuts, it is necessary to consider the following condition: $|\cos\vartheta_2| \leq H$, where H stands for the cosine of the minimum value of ϑ_2. By means of the analytical solutions of the kinematics, one derives the relations $x_2 \geq H_1 x_1$ and $x_2 \leq H_2 x_1$, with

$$H_1 = \sqrt{\frac{(1-H)(1-\cos\vartheta_1)}{(1+H)(1+\cos\vartheta_1)}} \tag{3.1}$$

and

$$H_2 = \sqrt{\frac{(1+H)(1-\cos\vartheta_1)}{(1-H)(1+\cos\vartheta_1)}}. \tag{3.2}$$

As can be easily seen, for $H \neq 0$ it is always $H_2 \geq H_1$. Moreover, we always assume $\cos\vartheta_1^{\min} < \cos\vartheta_2^{\min}$, which in turn implies $H_2 > 1$ and $H_1 < 1$. The conditions imposed by cuts on the scattering angles can be therefore synthesized as $H_1 x_1 \leq x_2 \leq H_2 x_1$.

Cut on the maximum acollinearity angle

Let us consider the effect ascribed to a different amount of electromagnetic radiation emitted by the incoming electron and positron, i.e., $x_1 \neq x_2$. As already stated, the case $x_1 \neq x_2$ corresponds to a situation in which the center of mass of the reaction is boosted with respect to the laboratory frame. Consequently, the final-state fermions are not produced back to back; i.e., an acollinearity is generated. Denoting with ζ_0 the maximum allowed acollinearity angle, we have to distinguish the two regions $x_1 < x_2$ and $x_1 > x_2$. In the first case ($x_1 < x_2$), if $\vartheta_1 < \zeta_0$, the cut has no effect because no boost can generate an acollinearity larger than ζ_0. When $\vartheta_1 \geq \zeta_0$ the following condition must be satisfied: $\vartheta_2 \leq \pi - \vartheta_1 + \zeta_0$. Introducing the notation $B = \cos(\vartheta_1 - \zeta_0)$ and using the analytical solutions (2.1)–(2.3) of the kinematics, one has the inequality $x_2 \leq K_2 x_1$, where

$$K_2 = \sqrt{\frac{(1-\cos\vartheta_1)(1+B)}{(1+\cos\vartheta_1)(1-B)}}. \tag{3.3}$$

In the second case ($x_1 > x_2$), if $\vartheta_1 > \pi - \zeta_0$ the cut has no effect. When $\vartheta_1 \leq \pi - \zeta_0$ it is necessary to consider the condition $\vartheta_2 \geq \pi - \vartheta_1 - \zeta_0$, which is equivalent to $x_2 \geq K_1 x_1$, where

$$K_1 = \sqrt{\frac{(1-\cos\vartheta_1)(1+A)}{(1+\cos\vartheta_1)(1-A)}}, \tag{3.4}$$

with the notation $A = \cos(\vartheta_1 + \zeta_0)$. A cut on the maximum acollinearity therefore requires $K_1 x_1 \leq x_2 \leq K_2 x_1$.

Cut on the invariant mass or the energy thresholds of the outgoing fermions

Generally, one can require a cut s_0 on the minimum invariant mass of the final fermion pair $f\bar{f}$ by setting $x_1 x_2 > \varepsilon = s_0/s$, where $s = 4E^2$. Alternatively, one can impose a cut on the energy thresholds of the outgoing fermions by requiring $E_{1,2} \geq E_0$ (we assume that $E^f_{\min} = E^{\bar{f}}_{\min}$). We have adopted an approximated procedure and implemented an energy-threshold cut as an invariant-mass cut by setting $s_0 = 2E_0\sqrt{s}$. The two kinds of cuts differ because an energy-threshold cut allows for hard noncollinear photons which are excluded by the corresponding invariant-mass cut. However, initial-state hard photons are suppressed in the Z^0 peak region; moreover, in a realistic setup an energy or invariant-mass cut is usually accompanied by an acollinearity cut, which, suppressing hard noncollinear radiation, almost eliminates the difference.

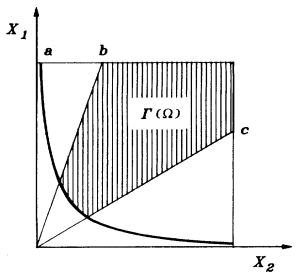

FIG. 2. Effect of realistic experimental cuts on the initial-state radiation phase space. The variables x_1, x_2 give the energies of the colliding particles as $x_{1,2}E$. The restrictions imposed by a cut on the invariant mass (a), on the scattering angles, and on the maximum acollinearity (b, c) are shown with the resulting allowed portion of the phase space $\Gamma(\Omega)$.

To conclude this section, the portion of initial-state radiation phase space allowed by realistic cuts is in general the region $\Gamma(\Omega)$ shown in Fig. 2, defined as the intersection of the regions delimited by the various experimental constraints, i.e.,

$$x_1 x_2 \geq s_0/s,$$
$$x_2 \leq K^+ x_1,$$
$$x_2 \geq K^- x_1,$$

where $K^+ = \min\{H_2, K_2\}$ and $K^- = \max\{H_1, K_1\}$. As shown in Sec. VI, once the phase-space region allowed by cuts is known, the treatment of the initial-state QED corrections in the framework of the SF can be analytically worked out in order to increase the accuracy of the required multidimensional numerical integrations.

IV. FINAL-STATE RADIATION WITH REALISTIC CUTS

In this section we will consider the correction coming from final-state radiation in presence of realistic kinematical cuts by recalling analytic $O(\alpha)$ results obtained in Refs. [11, 18] in order to improve the treatment adopted in Ref. [9] in the context of the fit program discussed in the Introduction. When no cuts at all are applied, the correction amounts to the factor $\frac{3}{4}\frac{\alpha}{\pi}Q_f^2$ for the total cross section, while the forward-backward asymmetry remains unchanged. If we assume that an invariant-mass cut such as $M^2(\bar{f}f) > \mu_f^2$ ($\mu_f^2 \leq s_0$) is present, the following correction factors have to be included [11]:

$$\delta^{fs}_{F+B} = \frac{\alpha}{\pi} Q_f^2 \Big\{ -\left[x + \tfrac{1}{2}x^2 + 2\ln(1-x)\right] \ln\frac{m_f^2}{s} + x\left(1+\tfrac{1}{2}x\right)\ln x + 2\ln(1-x)(\ln x - 1) + 2\,\mathrm{Li}_2(x)\Big\}, \tag{4.1}$$

$$\delta^{fs}_{F-B} = \frac{\alpha}{\pi} Q_f^2 \Big\{ -\left[x + \tfrac{1}{2}x^2 + 2\ln(1-x)\right] \ln\frac{m_f^2}{s} + 2\ln(1-x)(\ln x - 1) - 2x + 2\,\mathrm{Li}_2(x)\Big\}, \tag{4.2}$$

where $x = \mu_f^2/s$ and $(F \pm B)$ denotes the forward $\pm$ backward cross sections. When the initial-state radiation is switched on then, in the definition of the variable x, s has to be replaced by $\hat{s}$, $\hat{s}$ being the invariant mass of the event after initial-state radiation, $\hat{s} = x_1 x_2 s$.

In addition to an invariant-mass cut, also acollinearity and/or energy-threshold cuts can be treated analytically. The expressions for the corresponding $O(\alpha)$ correction factors were derived in [11] by integrating the full matrix element of the process $e^+e^- \to f\bar{f}\gamma$ (with γ emitted from the final states). They are too lengthy to be displayed here, but they are explicitly reported in [11]. Whereas at the level of initial-state radiation a cut on the angular acceptance of the antifermion can be represented as an acollinearity cut, at the level of final-state radiation it cannot be treated analytically. Some numerical checks [11] have, however, shown that its contribution, for realistic acollinearity cuts, is small, of order 1–2 per mill. Of course, in the case of a totally inclusive setup, the correction factors with cuts correctly recover the results for extrapolated situation discussed at the beginning of this section. In Ref. [11] the above correction factors were derived exactly at $O(\alpha)$, neglecting resummation of higher-order contributions. However, for realistic observables higher-order final-state effects could become important and a procedure of resummation should be introduced. Some possible recipes are proposed and compared in Sec. V.

When considering Bhabha scattering one is also faced with the problem of the calorimetric measurement for electrons. Actually, it is experimentally impossible to discriminate between a single electron in a calorimeter and an electron plus a hard photon sufficiently collinear with the electron, and therefore the two possible final states provide indistinguishable experimental configurations. What is detected is an *electromagnetic jet* of semiaperture δ_c, where δ_c is an experimental parameter describing the resolution power of the calorimeter. In our approach this effect is accounted for by adding to the $O(\alpha)$ part of the final-state QED correction the contribution due to an hard photon of energy fraction greater then $1-x$, where x is s_0/s for an invariant-mass cut and $2E_0/\sqrt{s}$ for an energy-threshold cut, and collinear with the final fermion within an angle $0 \le \vartheta_\gamma \le \delta_c$. For electrons in the energy regime of LEP/SLC the contribution reads [18]

$$F^{\pm}_{\mathrm{coll}} = 2\frac{\alpha}{\pi}C,$$
$$C = -\ln(1-x)\left[\ln\left(1+r^2x^2\right) - 1\right] + \left[\frac{1}{4} - \left(1 - \frac{1}{2}(1-x)\right)^2\right]\ln\left(1+r^2x^2\right) + \frac{\pi^2}{3} + \frac{9}{4} - \frac{5}{2}(1-x) + \frac{1}{4}(1-x)^2 + 2\ln x\ln(1-x) + 2\mathrm{Li}_2(1-x), \tag{4.3}$$

where

$$r = \frac{\delta_c\sqrt{s}}{2m_e}, \tag{4.4}$$

m_e being the electron mass. The approximation $\delta_c \ll 1$ rad and $r \gg 1$ is assumed since these conditions are very well satisfied at LEP/SLC. Equation (4.3) is a good approximation of the general formula derived in [18] and also reported in Appendix A, which holds for arbitrary values of r and of the calorimetric threshold. Taking into account the effect of final-state hard collinear photons is equivalent to adopting two different algorithms in computing the final-state QED correction, namely, an exclusive algorithm for hard noncollinear photons such that the invariant mass of the final $\bar{f}f$ pair or the energy of each fermion is above a given threshold and a *jet* algorithm for photons such that the system $\bar{f}f\gamma$ is degenerate with a system $\bar{f}f$. From this point of view the QED final state is equivalent to a QCD final state, where it is in principle impossible to tag each *parton* inside the hadronic jet. As a last remark, we stress that the effect of the calorimetric measurement depends very critically on the energy or invariant-mass threshold. Its numerical contribution is of order 1 per mill at thresholds around 1 GeV, but raises to order 1 percent at, say, 10 GeV [1].

V. FORMULATION FOR s-CHANNEL OBSERVABLES

In this section we discuss the formalism adopted for the calculation of the QED corrections to physical observables (total cross section and forward-backward asymmetry) in the case of s-channel annihilation over a fully extrapolated experimental setup and a realistic one. In the extrapolated situation, the initial-state radiation can be effectively accounted for by adopting the so-called radiator approach, which amounts to write down a *corrected* cross section in the form [4, 5]

$$\sigma_c^{\pm}(s) = \int_0^{1-\epsilon} dx H(x,s)\sigma_0^{\pm}\Big((1-x)s\Big), \tag{5.1}$$

where

$$\sigma_0^{\pm}(s) = 2\pi\left[\int_0^1 \pm \int_{-1}^0\right] d\cos\vartheta \frac{d\sigma_0}{d\cos\vartheta} \tag{5.2}$$

and $d\sigma_0/d\cos\vartheta$ is the differential cross section. From the point of view of QED corrections, $d\sigma_0/d\cos\vartheta$ is an arbitrary kernel. However, in order to compare theoretical cross sections and asymmetries with the experimental

ones and derive from a fit to the data limits on parameters such as m_t, m_H, and α_s, weak loops and form factors and QCD corrections are fundamental ingredients for the calculation of the kernel cross section. Actually in Ref. [1] $d\sigma_0/d\cos\vartheta$ has been computed strictly within the MSM as far as pure weak [6, 7], strong [20], and recently proposed higher-order corrections [21] are concerned.

$H(x,s)$ is the radiator which takes into account soft-photon exponentiation and hard-photon emission up to $O(\alpha^2)$ (see later for its definition) and is given by

$$H(x,s) = (1+\delta+\delta_p)\,\beta\,x^{\beta-1} - \tfrac{1}{2}\beta\,(2-x) + \tfrac{1}{8}\beta^2 \times\Big\{(2-x)\,[3\ln(1-x) - 4\ln x] - \frac{4}{x}\ln(1-x) - 6 + x\Big\}. \tag{5.3}$$

The variable x gives the total amount of energy emitted by the initial state and is linked to x_1 and x_2 by the relation $x = 1 - x_1x_2$. In Eq. (5.3) the meaning of the symbols is

$$\beta = 2\frac{\alpha}{\pi}(L-1), \qquad L = \ln\frac{s}{m_e^2}, \tag{5.4}$$

$$\delta = \frac{\alpha}{\pi}\left(\tfrac{3}{2}L + \tfrac{\pi^2}{3} - 2\right) + \left(\frac{\alpha}{\pi}\right)^2\left\{\left(\tfrac{9}{8} - \tfrac{\pi^2}{3}\right)L^2 + \left[-\tfrac{45}{16} + \tfrac{11}{12}\pi^2 + 3\zeta(3)\right]L - \tfrac{9}{2}\zeta(3) - \pi^2\ln 2 + \tfrac{19}{144}\pi^2 + \tfrac{57}{12}\right\}, \tag{5.5}$$

$$\delta_p = \left(\frac{\alpha}{\pi}\right)^2\left[\sum_{l=e,\mu}\delta_p^l + \sum_h \delta_p^h\right]. \tag{5.6}$$

The factor δ reabsorbs the next-to-leading terms up to $O(\alpha^2)$ which come from the electron form factor and soft bremsstrahlung and represent the universal part of the initial-state QED corrections. δ_p^l and δ_p^h refer, respectively, to lepton and hadron pair production from the initial state. For energies around the Z^0 peak they have the expressions [22]

$$\delta_p^l = \left[\tfrac{1}{2}L_{pl}^2 - \tfrac{\pi^2}{3} + \left(\ln 4 - \tfrac{5}{3}\right)L_{pl} + \tfrac{1}{2}\ln^2 4 - \tfrac{5}{3}\ln 4 + \tfrac{28}{9}\right]\left(\tfrac{2}{3}L_z + \tfrac{1}{2}\right) + \left(\tfrac{2}{3}L_z^2 - \tfrac{7}{12}\right)\ln\frac{s}{m_l^2} + \tfrac{4}{9}L_z^3 + \tfrac{2}{3}\zeta(3) + \tfrac{5}{8}, \tag{5.7}$$

$$\delta_p^h = \left[4\left(\tfrac{1}{2}L_{ph}^2 - \frac{\pi^2}{6}\right) - 8.31\,L_{ph} + 13.1\right]\left(\tfrac{2}{3}L_z + \tfrac{1}{2}\right) + (4L_{ph} - 8.31)\left(\tfrac{2}{3}L_z^2 - \tfrac{7}{12}\right) + 4\left[\tfrac{4}{9}L_z^3 + \tfrac{2}{3}\zeta(3) + \tfrac{5}{8}\right], \tag{5.8}$$

with $L_{pf} = \ln(s/4m_f^2)$ and $L_z = \ln(2\Gamma_z/\sqrt{s})$. For the hadrons we used $h = \pi$, K, η, ρ, and ω. The parameter ε is defined by

$$\varepsilon = 4\frac{m_f^2}{s} \tag{5.9}$$

when including the whole photon phase space. It can also be used to account for a cut on the invariant mass after initial-state radiation by simply replacing $4m_f^2$ with a cut s_0.

Having defined σ_c^- and σ_c^+, the forward-backward asymmetry is computed as [23]

$$A_{FB}(s) = \frac{\sigma_c^-(s)}{\sigma_c^+(s)}. \tag{5.10}$$

For a completely inclusive setup, the final-state radiation can be easily included by incorporating a factor $1 + \delta_{F\pm B}^{fs}$ in the kernel cross section. The expressions for $\delta_{F\pm B}^{fs}$ are given by Eqs. (4.1) and (4.2).

Let us now consider the more involved case of a realistic experimental setup. For such a configuration the starting point is the following formula, based on factorization theorems of mass and collinear singularities [24], for the corrected $F \pm B$ cross section in the laboratory frame [9]:

$$\sigma_c^{\pm}(s) = \int_{R^{\pm}} d\Omega \int_{\Gamma(\Omega)} dx_1 dx_2 D(x_1,s)D(x_2,s)J(x_1,x_2,\vartheta_1)\frac{d\sigma_0}{d\Omega}(\hat{s}(x_1,x_2),\hat{t}(x_1,x_2,\vartheta_1))F_{\rm cut}^{\pm}(\hat{s}(x_1,x_2)). \tag{5.11}$$

The angular integration region is

$$\int_{R^{\pm}} d\Omega = \int_0^{2\pi} d\varphi\left[\int_0^{\cos\vartheta_{\min}} \pm \int_{\cos(\pi-\vartheta_{\min})}^{0}\right] d\cos\vartheta_1,$$

where φ and ϑ_1 are the azimuthal and polar angle of the scattered fermion. The region $\Gamma(\Omega)$ is shown in Fig. 2. At present, the angular integration is performed over a symmetric angular setup, but the generalization to an arbitrary region is straightforward. With respect to the

formulation given in Ref. [9], the region of the initial-state radiation phase space allowed by cuts is analytically delimited and the description of the final-state radiation is improved by the results derived in [11, 18] and summarized in Sec. IV. The meaning of the terms entering Eq. (5.11) is the following. $D(x_{1(2)}, s)$ is the structure function of the incoming lepton (antilepton), representing the probability that the electron (positron) retains a fraction $x_{1(2)}$ of its original momentum. Its expression includes soft-photon resummation and hard-photon effects up to $O(\alpha^2)$, and reads [5]

$$D(x,s) = \Delta' \frac{1}{2}\beta(1-x)^{\frac{1}{2}\beta-1} - \frac{1}{4}\beta(1+x) + \frac{1}{32}\beta^2\Big[-4(1+x)\ln(1-x) + 3(1+x)\ln x - 4\frac{\ln x}{1-x} - 5 - x\Big],$$
$$\Delta'^2 = 1 + \delta + \delta_p + \frac{\pi^2}{24}\beta^2, \tag{5.12}$$

with δ, δ_p, and β given in Sec. IV. $d\sigma_0/d\Omega$ is the kernel cross section. As stated above, weak and QCD corrections together with final fermion-mass effects have to be included in the kernel cross section for a reliable and completely realistic description of the physical observables. $\hat{s}$ and $\hat{t}$ are the radiatively reduced Mandelstam variables depending on the longitudinal-momentum fractions x_1, x_2 and on the fermion-scattering angle ϑ_1. $J(x_1, x_2, \vartheta_1)$ is the Jacobian of the transformation from the center of mass to the laboratory frame, i.e.,

$$\frac{d}{d\cos\vartheta_1} = \left|\frac{d\cos\vartheta_{\text{c.m.}}}{d\cos\vartheta_1}\right| \frac{d}{d\cos\vartheta_{\text{c.m.}}}. \tag{5.13}$$

In the ultrarelativistic approximation its expression reads

$$J(x_1, x_2, \vartheta_1) = \frac{x_1 x_2}{\left(x_1 \sin^2\frac{\vartheta_1}{2} + x_2 \cos^2\frac{\vartheta_1}{2}\right)^2}. \tag{5.14}$$

$F^{\pm}_{\text{cut}}(s)$ is the final-state QED correction for the $F \pm B$ cross section in the presence of experimental cuts. It is worth noting that the final-state correction is not exactly implemented, since the correction is not exactly factorized over the lowest-order cross section. However, the nonfactorized terms are numerically small by themselves, and moreover they exactly cancel when the cross section is integrated over a symmetric angular setup. In order to take into account the final-state radiation exactly at $O(\alpha)$, we should set $F^{\pm}_{\text{cut}}(s) = 1 + \delta^{fsc}_{F\pm B}$, where $\delta^{fsc}_{F\pm B}$ is the correction factor taking into account the acollinearity and/or energy-threshold cut derived in Ref. [11]. But in a realistic setup higher-order final-state QED corrections could become important, and so it is necessary to introduce a procedure of resummation of higher-order effect such as the exponentiation. As already discussed in Ref. [1], from Eqs. (4.1) and (4.2) it can be seen that a leading term can be defined as

$$F^{l}_{\text{cut}}(s) = -2\frac{\alpha}{\pi}Q_f^2 \ln(1 - s_0/s)\left[\ln\left(\frac{m_f^2}{s}\right) + 1\right]. \tag{5.15}$$

Renormalization-group arguments lead to state that such a leading term should be exponentiated, which is of no practical importance at low thresholds, but could give sizable effects at high thresholds. By defining

$$F^{\pm}_{\text{cut,r}}(s) = F^{\pm}_{\text{cut},\alpha}(s) - F^{l}_{\text{cut}}(s), \tag{5.16}$$

the leading-term resummation can be implemented as follows:

$$F^{\pm}_{\text{cut}}(s) = \exp[F^{l}_{\text{cut}}(s)]\Big[1 + F^{\pm}_{\text{cut,r}}(s) - F^{\pm}_{\text{cut,r}}(s)F^{l}_{\text{cut}}(s)\Big], \tag{5.17}$$

where spurious terms $F^{l}_{\text{cut}}(s)F^{\pm}_{\text{cut,r}}(s)$ are confined at least at $O(\alpha^3)$. Indeed, several prescriptions for treating the final-state correction are possible, all equivalent at $O(\alpha)$. One reasonable recipe, different from the one we follow, could be defining the leading term in a different way. For instance, in the presence of an acollinearity cut the infrared logarithm could be defined as

$$l = \ln(1 - x), \tag{5.18}$$

where x is given by

$$x = \max(s_0/s, y_T), \tag{5.19}$$

y_T being

$$y_T = \frac{1 - \sin(\zeta/2)}{1 + \sin(\zeta/2)} \tag{5.20}$$

and ζ the maximum acollinearity allowed. Another possibility could be exponentiating the full $O(\alpha)$ contribution $F^{\pm}_{\text{cut},\alpha}$; albeit, there is no guarantee that the experimental cut-dependent terms do exponentiate; in this case spurious terms appear already at $O(\alpha^2)$. Alternatively, one could choose to factorize only a leading $O(\alpha)$ term and simply add the $O(\alpha)$ correction due to the acollinearity cut (this simulates the choice of the authors of [12]). This choice seems to us less natural than the first ones, because, apart from very small terms, the final-state correction factorizes over the *Born* cross section, but it is equivalent to them at $O(\alpha)$. It must be noted that at the Z^0 peak all these choices are compatible at the per mill level, but a few GeV away from the peak and in presence of severe experimental cuts they can differ by several per mill [1]. The differences can become more marked in the case of large-angle Bhabha scattering because of the presence of t-channel contributions. However, in view of the present level of experimental accuracy, this can be considered as a matter of principle with no phenomenological relevance, because the *theoretical error* ascribed to the higher-order QED final-state uncertainty is one order of magnitude smaller than the experimental error.

The initial–final-state interference is not taken into account in the master formula (5.11). In order to estimate its contribution the following procedure has been adopted. Since the largest contribution comes from the interference of soft photons, the soft-approximation formulas quoted in [19] have been used. Moreover, only the leading terms have been taken into account. In the approximation stated above the interference contribution

to the corrected cross sections reads

$$\sigma_{\rm int}^{\pm(i)}(s) = \int_{R^\pm} d\Omega \frac{d\sigma_0^{(i)}}{d\Omega} \Big[C_{\rm infra}^{(i)}(\Delta,\beta,\beta_f,\beta_{\rm int}) - C_{\rm infra}^{(i)}(\Delta,0,0,\beta_{\rm int}) \Big], \quad (5.21)$$

where $\Delta = \max(1 - s_0/s, y_T)$, β is given in Sec. IV, $\beta_f = 2\alpha/\pi[\ln(s/m_f^2) - 1]$, m_f being the mass of the final-state fermion, and $\beta_{\rm int} = 4\alpha/\pi \ln(\tan\vartheta/2)$. Since the interference contribution is not universal, it has been needed to split the cross section into its separate contributions according to [19], where also the expressions for $C_{\rm infra}^{(i)}$ can be found. Some numerical checks in several realistic situations have shown that the interference contribution is of order 1 per mill at the resonance, raising to a few per mill far from it. Also, the correction to the asymmetry, which could be in principle more sizable, has revealed to be contained in few units times 10^{-3}, always far from the peak. In view of the present experimental accuracy and the final-state theoretical uncertainty discussed above, we concluded that it can be safely neglected in the software implementation.

As a last feature of the approach, we recall [1, 2] that for fitting realistic observables a lot of CPU time can be saved by molding the following expression for the running of α with the scale s:

$$\begin{aligned} \alpha(s) &= a_0 + a_1 \ln(\mu^2/s) + a_2 \frac{s}{m_t^2}, \\ a_0 &= 0.743635313782749 \times 10^{-2}, \\ a_1 &= -0.410825034114194 \times 10^{-4}, \\ \mu^2 &= 3.15676857855315\,{\rm GeV}^2, \\ a_2 &= 0.325766572488072 \times 10^{-6}, \end{aligned} \quad (5.22)$$

which reproduces the exact [7] expression, including the parametrization for the hadronic contributions as in Ref. [25], to high accuracy in the range $1\,{\rm GeV} < E_{\rm beam} < 50\,{\rm GeV}$ and $10\,{\rm GeV} < m_t < 350\,{\rm GeV}$. As will be seen, this procedure of molding some simple expression for α is crucial for the application of the approach to large-angle Bhabha scattering.

VI. REDUCTION TO "GEOMETRICAL" INTEGRALS

The master formula (5.11) proposed in the previous section has to be manipulated a lot in order to extract stable and fast numerical predictions. Actually, the formula as it stands exhibits several computational problems. First of all, it is in the form of a triple integration. Second, the electron structure function has an infrared singularity in $x = 1$ which is integrable but not square integrable, a fact which renders the numerical integration cumbersome. Last, the kernel cross section exhibits the Coulombic singularity for $s \to 0$; this feature is not a severe problem for an s-channel annihilation, but becomes a serious difficulty in the presence of t-channel processes.

In order to solve these computational problems the following strategy has been adopted. The corrections due to kinematical effects and to an acollinearity and/or acceptance cut, which from now on will be called "geometric" corrections, albeit important, are a small contribution as compared to the QED correction due to an invariant-mass cut alone. Let us define $\sigma_{\rm cut}^\pm$ as

$$\sigma_{\rm cut}^\pm(s) = \int_{R^\pm} d\Omega \frac{d\sigma_0}{d\Omega}\Big(\hat{s}(1,1), \hat{t}(1,1,\vartheta_1)\Big), \quad (6.1)$$

where $\hat{s}(1,1)$ and $\hat{t}(1,1,\vartheta_1)$ are the lowest-order Mandelstam variables, $s = E_{\rm c.m.}^2$, and $t = -\frac{s}{2}(1 - \cos\vartheta_1)$. Then a *regulating cross section* can be conveniently defined as

$$\sigma_r^\pm(s) = \int_0^{1-s_0/s} dx H(x,s) \sigma_{\rm cut}^\pm\Big((1-x)s\Big) \times F_{\rm cut}^\pm\Big((1-x)s\Big), \quad (6.2)$$

where $H(x,s)$ is the radiator introduced in the previous section and linked to the electron structure function by the relation

$$H(x,s) = \int_{1-x}^1 \frac{dz}{z} D(z,s) D\Big(\frac{1-x}{z}, s\Big). \quad (6.3)$$

The cross section $\sigma_r^\pm(s)$ has some good features. The first one is that it provides the bulk of the corrected cross section. It is a one-dimensional integral which can be reduced to a large analytical term plus a correction whose numerical computation is very fast and accurate. Namely, we can rewrite Eq. (6.2) as [1]

$$\begin{aligned} \sigma_r^\pm(s) = \bar{x} &\int_0^1 dx\, [f(x's) - f(s)]\, H(1-x',s) \\ &+ \bar{x}' \int_0^1 dx\, [f(x''s) - f(\varepsilon s)]\, H(1-x'',s) \\ &+ f(s)\, P_H(\bar{x},s) + f(\varepsilon s)\, [P_H(x_M,s) - P_H(\bar{x},s)], \end{aligned} \quad (6.4)$$

where

$$\begin{aligned} f(x) &= \sigma_{\rm cut}^\pm(x) F_{\rm cut}^\pm(x), \\ x_M &= 1 - \varepsilon, \qquad x' = 1 - \bar{x}x, \\ \bar{x}' &= 1 - \bar{x} - \varepsilon, \qquad x'' = 1 - \bar{x} - \bar{x}'x. \end{aligned}$$

$P_H(x,s)$ is the primitive of the radiator $H(z,s)$ defined as

$$\begin{aligned} P_H(x,s) &= \int_0^x dz\, H(z,s) \\ &= (\delta + \delta_p)x^\beta - \frac{1}{2}\beta\left(x - \frac{1}{2}x^2\right) \\ &\quad + \frac{1}{8}\beta^2\Big[-\frac{5}{2}x + \frac{1}{4}x^2 - 6\ln(1-x) + 6x\ln(1-x) - \frac{3}{2}x^2\ln(1-x) + \frac{3}{2}\ln(1-x) + 8x\ln x + 2x^2\ln x + 4{\rm Li}_2(x)\Big]. \end{aligned} \quad (6.5)$$

In Eq. (6.4) we have splitted the integration and performed the relative subtractions in order to increase the accuracy in the one-dimensional numerical integration. The first subtraction is needed because of the behavior of $H(x,s)$ for $x \sim 0$; the second is required to regularize the behavior of the integrand at the thresholds. If we require $\hat{s} > s_0$, then $\varepsilon = s_0/s$. The parameter $\overline{x}$ is used for splitting the integration, and in our calculation we used $\overline{x} = 0.98 - \varepsilon$.

For a pure s-channel annihilation $\sigma^{\pm}_{\rm cut}(s)$ is analytically integrated in a straightforward way, which is of some importance for the F-B cross section near the Z^0 peak, where it becomes very small due to a fine cancellation of the F and B contributions.

In order to take advantage of the definition of $\sigma^{\pm}_r(s)$, the corrected cross section can be written as

$$\sigma^{\pm}_c(s) = \sigma^{\pm}_r(s) - \left[\sigma^{\pm}_r(s) - \sigma^{\pm}_c(s)\right], \tag{6.6}$$

where now the difference between $\sigma^{\pm}_r(s)$ and $\sigma^{\pm}_c(s)$ exhibits a structure of singularity much more simple that $\sigma^{\pm}_c(s)$ itself. This feature can be exploited if such a difference is worked out as much as possible analytically. Taking into account that in the language of structure functions $\sigma^{\pm}_r(s)$ can be written as

$$\sigma^{\pm}_r(s) = \int_{R^{\pm}} d\Omega \int_{\bar{\Gamma}(\Omega)} dx_1 dx_2 D(x_1,s) D(x_2,s) \times \frac{d\sigma_0}{d\Omega}\left(x_1x_2s, x_1x_2t\right), \tag{6.7}$$

where $\bar{\Gamma}(\Omega)$ is the radiation phase space with no experimental cuts but an invariant-mass one, after some simple algebra the corrected cross section can be written as

$$\sigma^{\pm}_c(s) = \sigma^{\pm}_r(s) - \int_{R^{\pm}} d\Omega \left\{ \int_{\Gamma(\Omega)} dx_1 dx_2 D(x_1,s) D(x_2,s) \frac{d\sigma_{\Delta}}{d\Omega}(x_1,x_2,\vartheta_1) F^{\pm}_{\rm cut}(x_1x_2s) + \int_{C(\Gamma(\Omega))} dx_1 dx_2 D(x_1,s) D(x_2,s) \frac{d\sigma_0}{d\Omega}\left(x_1x_2s, x_1x_2t\right) F^{\pm}_{\rm cut}(x_1x_2s) \right\}, \tag{6.8}$$

where

$$\frac{d\sigma_{\Delta}}{d\Omega}(x_1,x_2,\vartheta_1) = \frac{d\sigma_0}{d\Omega}\left(x_1x_2s, x_1x_2t\right) - J(x_1,x_2,\vartheta_1) \frac{d\sigma_0}{d\Omega}\left(\hat{s}(x_1,x_2), \hat{t}(x_1,x_2,\vartheta_1)\right).$$

The integration region in the (x_1,x_2) plane in the last integral, $C(\Gamma(\Omega))$, is defined by the relation $\bar{\Gamma}(\Omega) = \Gamma(\Omega) \cup C(\Gamma(\Omega))$ (see Fig. 2).

By definition $d\sigma_{\Delta}/d\Omega$ is zero for $x_1 = x_2$. This allows to split the space $\Gamma(\Omega)$ into two regions where only one singularity appears. Analogously, $C(\Gamma(\Omega))$ is by definition split into a region $(x_2 \geq x_1)$ where only the singularity $x_2 = 1$ is present and a region $(x_1 \geq x_2)$ where only the other singularity $x_1 = 1$ appears. Over each of these regions the singularity due to the structure function has been regularized by means of the pole subtraction procedure. For instance, in the part of the region $\Gamma^+(\Omega)$, where $x_1 \leq x_2$, we have

$$\int_{\Gamma^+(\Omega)} dx_1 dx_2 D(x_1,s) D(x_2,s) \frac{d\sigma_{\Delta}}{d\Omega}\left(x_1,x_2,\vartheta_1\right) = \int_{\Gamma^+(\Omega)} dx_1 dx_2 D(x_1,s) D(x_2,s) \left[\frac{d\sigma_{\Delta}}{d\Omega}\left(x_1,x_2,\vartheta_1\right) - \frac{d\sigma_{\Delta}}{d\Omega}\left(x_1,1,\vartheta_1\right)\right] + \int_{\xi_2}^1 dx_1 \left[P_D\left(a^+(x_1,\varepsilon(s))\right) - P_D\left(b^+(x_1)\right)\right] D(x_1) \frac{d\sigma_{\Delta}}{d\Omega}\left(x_1,1,\vartheta_1\right), \tag{6.9}$$

where $\xi_2 = \sqrt{\frac{\varepsilon(s)}{K^+}}$, $a^+(x_1,\varepsilon(s)) = \max\left(x_1, \frac{\varepsilon(s)}{x_1}\right)$, $b^+(x_1) = \min(1, K^+x_1)$. $P_D(z)$ is the primitive of the structure function defined as

$$\begin{aligned} P_D(z) &= \int_z^1 dx D(x) \\ &= \Delta'(1-z)^{\beta/2} + \frac{1}{4}\beta\left(-\frac{3}{2} + z + \frac{z^2}{2}\right) \\ &\quad + \frac{1}{32}\beta^2\left[-\frac{9}{4} + \frac{4}{6}\pi^2 - 4{\rm Li}_2(z) + 2z + \frac{z^2}{4} + 2\left(z^2+2z-3\right)\ln(1-z) - 4\ln z \ln(1-z) - 3\left(\frac{z^2}{2}+z\right)\ln z\right]. \end{aligned} \tag{6.10}$$

Analogously, in the part of the region $C^+(\Gamma(\Omega))$, where $x_1 \leq x_2$, we have

$$\int_{C^+(\Gamma(\Omega))} dx_1 dx_2 D(x_1,s) D(x_2,s) \frac{d\sigma_0}{d\Omega}\left(x_1 x_2 s, x_1 x_2 t\right)$$

$$= \int_{C^+(\Gamma(\Omega))} dx_1 dx_2 D(x_1,s) D(x_2,s) \left[\frac{d\sigma_0}{d\Omega}\left(x_1, x_2, \vartheta_1\right) - \frac{d\sigma_0}{d\Omega}\left(x_1, 1, \vartheta_1\right)\right]$$
$$+ \int_{\varepsilon(s)}^{1/K^+} dx_1 P_D\left(c^+(x_1, \varepsilon(s))\right) D(x_1) \frac{d\sigma_0}{d\Omega}\left(x_1, 1, \vartheta_1\right), \tag{6.11}$$

where $c^+(x_1,\varepsilon(s)) = \max\left(K^+ x_1, \frac{\varepsilon(s)}{x_1}\right)$. For the sake of simplicity we understand the final-state radiation correction to be included in the kernel cross sections. Analogously, similar decompositions can be carried out for the regions $\Gamma^-(\Omega)$ and $C^-(\Gamma(\Omega))$, where $x_1 \geq x_2$. In so doing, the original three-dimensional integrals (6.8) are reduced to two double and two triple integrations for both $\Gamma^{+,-}(\Omega)$ and $C^{+,-}(\Gamma(\Omega))$, characterized by the fact that the resulting three-dimensional integrals are free of singularities and numerically small as compared to the two-dimensional ones.

The double integrations coming from the complementary spaces $C^+(\Gamma(\Omega))$ and $C^-(\Gamma(\Omega))$ have been further regularized, since, albeit shielded, they are again sensitive to the infrared singularity for x near 1 and exhibit the Coulombic pole close to the invariant-mass boundary. Take, for instance, the region $C^+(\Gamma(\Omega))$ previously considered. First of all, we have split the interval $\left[\varepsilon, \frac{1}{K^+}\right]$ in the two intervals $\left[\min\left(\varepsilon, \frac{1}{2}\right), \min\left(\frac{1}{K^+}, \frac{1}{2}\right)\right]$ and $\left[\max\left(\varepsilon, \frac{1}{2}\right), \max\left(\frac{1}{K^+}, \frac{1}{2}\right)\right]$. Introducing the notations $a = \min\left(\varepsilon, \frac{1}{2}\right)$, $b = \min\left(\frac{1}{K^+}, \frac{1}{2}\right)$, $c = \max\left(\varepsilon, \frac{1}{2}\right)$, $d = \max\left(\frac{1}{K^+}, \frac{1}{2}\right)$, and considering the photonic contribution $d\sigma_0^\gamma/d\Omega$ to the cross section (which is sensitive to the Coulombic pole), we regularize it in the first interval as follows:

$$\int_a^b dx_1 P_D\left(c^+(x_1,\varepsilon(s))\right) D(x_1) \frac{d\sigma_0^\gamma}{d\Omega}\left(x_1, 1, \vartheta_1\right)$$

$$= \int_a^b dx_1 \left[P_D\left(c^+(x_1,\varepsilon(s))\right) D(x_1) - D\left(\min\left\{\varepsilon, \frac{1}{2}\right\}\right)\right] \frac{d\sigma_0^\gamma}{d\Omega}\left(x_1, 1, \vartheta_1\right)$$
$$+ D\left(\min\left\{\varepsilon, \frac{1}{2}\right\}\right) \frac{d\sigma_0^\gamma}{d\Omega}\left(1, 1, \vartheta_1\right) \ln\left[\frac{\min\left\{\frac{1}{K^+}, \frac{1}{2}\right\}}{\min\left\{\varepsilon, \frac{1}{2}\right\}}\right]. \tag{6.12}$$

In the second interval the singularity due to the structure function can be regularized as

$$\int_c^d dx_1 P_D\left(c^+(x_1,\varepsilon(s))\right) D(x_1) \frac{d\sigma_0^\gamma}{d\Omega}\left(x_1, 1, \vartheta_1\right)$$

$$= \int_c^d dx_1 D(x_1) \left[P_D\left(c^+(x_1,\varepsilon(s))\right) \frac{d\sigma_0^\gamma}{d\Omega}\left(x_1, 1, \vartheta_1\right) - \frac{d\sigma_0^\gamma}{d\Omega}\left(d, 1, \vartheta_1\right)\right] + \frac{d\sigma_0^\gamma}{d\Omega}\left(d, 1, \vartheta_1\right)\left[P_D(c) - P_D(d)\right]. \tag{6.13}$$

This procedure allows to represent the largest part of the two-dimensional integrals over the complementary space as one-dimensional angular integrations. In order to obtain numerical stability, in the interval $[a,b]$ we have also performed the following integration-variable substitution: $dx_1 / x_1 = dy$.

To summarize the procedure described in this section, the corrected cross section is finally written as the sum of an analytical term plus a one-dimensional integral (which is the numerical residual of $\sigma_r^\pm$) plus one-, two-, and three-dimensional integrals coming from the geometric corrections. The relevant feature of the regularization procedure adopted is that a hierarchy of contributions is clearly pointed out, the higher the dimensionality of the integral the smaller being the contribution itself. This has as a first advantage that the prediction is numerically stable, and as a second advantage that when loosening the experimental cuts the geometric corrections become smaller and smaller, recovering in a natural way the inclusive limit previously discussed. As a non-negligible by-product, the third advantage is that, being the geometric corrections small, the geometric integrals reach an acceptable level of numerical stability without the need of requiring high numerical precision, thus allowing very

fast numerical computations.

The evaluation of QED corrections for s-channel observables as described in Secs. V and VI, properly interfaced with a library for weak [6, 7], QCD [20], and recently derived higher-order corrections [21], is implemented in the semianalytical program TOPAZ0 [1, 2]. In Ref. [1] numerical results of TOPAZ0 were compared with those obtained by ZFITTER [14] and ALIBABA [12] in several s-channel annihilations, for both extrapolated and realistic setup, showing a fully satisfactory agreement.

VII. LARGE-ANGLE BHABHA SCATTERING

This section is devoted to briefly showing how the formalism described in the previous sections can be applied to obtain a description for large-angle Bhabha scattering suitable for fitting purposes. Actually, as discussed in Ref. [1], if fast and high-precision numerical predictions for large-angle Bhabha scattering become available, direct fits to full Bhabha observables as measured by the LEP/SLC Collaborations can be performed without the need of performing the so called t-channel subtraction procedure usually employed by the experiments. Several authors tackled the Bhabha problem up to now and several codes (semianalytical and Monte Carlo codes) are available, both for large and small scattering angles [26]. The main difficulty in treating Bhabha scattering is that, in principle, due to the presence of t-channel processes, it is a two-scale problem. Some physical considerations can, however, help in solving the problem for the case of large-angle Bhabha scattering. Actually, one-photon t-channel exchange dominates the cross section at small angles ($\vartheta_1 \simeq 1^\circ$), whereas in the large-angle regime ($\vartheta_1 \geq 10^\circ$) the cross section is dominated by s-channel processes and one-photon t-channel exchange and its interference with Z^0 annihilation can become sizable, but only a few GeV under the peak. Moreover, at large scattering angles the scale t becomes of the same order of magnitude as s, so that Bhabha scattering at large angles can be approximated by considering it as a one-scale problem. This can be achieved by putting as $d\sigma_0/d\Omega(s,t)$ in the master formula the kernel cross section of Bhabha scattering, comprehensive of t-channel processes. In so doing the initial-final interference effect and the $O(\alpha)$ constants which come from the QED correction to t and s-t contributions are not correctly reproduced, but the error committed has to be rescaled to the percentage contribution of t and s-t terms to the cross section. In order to estimate their magnitude the initial-final interference contribution to the cross section, for t and s-t subprocesses, has been defined as

$$\sigma_{int}^{\pm(i)}(s) = \int_{R^\pm} d\Omega \frac{d\sigma_0^{(i)}}{d\Omega} \left[C_{\rm infra}^{(i)}(\Delta,\beta,\beta_f,\beta_{\rm int})(1+C_F^{(i)}) - C_{\rm infra}^{(i)}(\Delta,0,0,\beta_{\rm int}) \right], \quad (7.1)$$

where the factors $C_F^{(i)}$, which can be found in Ref. [19], take into account the difference between the constant terms implemented in the master formula and the right constant terms for these processes which, in the soft-photon approximation, come only from the electron form factor. Again, as for the s-channel case, this effect has been found to be small and hence neglected.

At this point the same regularization procedure as described above for pure s processes has been followed. An additional problem is due to the nontrivial running of the coupling constant α with the scale t. Actually, the exact expression for $\alpha(t)$ is rather complicated, thus preventing from integrating $d\sigma_0/d\Omega(s,t)$ over the scattering angle in order to define the regulating cross section $\sigma_r^\pm(s)$. Again, the problem has been solved by molding the exact result [7] for $\alpha(t)$ by the much simpler expression [1, 2]

$$\begin{aligned} \alpha(t) &= a_0 - a_1 \ln\left(\frac{\mu^2}{-t}\right) + a_2 \frac{t}{m_t^2}, \\ a_0 &= 0.74595047 \times 10^{-2}, \\ a_1 &= 0.43344392 \times 10^{-4}, \\ \mu^2 &= 7.3526544\ \text{GeV}^2, \\ a_2 &= -0.81220219 \times 10^{-6}, \end{aligned} \quad (7.2)$$

where, albeit small, a dependence on m_t has been taken into account. The coefficients have been fitted for t and m_t in the range $-8000\ \text{GeV}^2 \leq t \leq -500\ \text{GeV}^2$ and $20\,\text{GeV} \leq m_t \leq 250\,\text{GeV}$, which, at the resonance, nearly corresponds to the angular setup $30^\circ \leq \vartheta_1 \leq 150^\circ$, but some numerical checks have shown that the same fitting coefficients work also for the angular setup $10^\circ \leq \vartheta_1 \leq 170^\circ$ at a very high accuracy.

The molded formula is crucial for the application of the approach to Bhabha scattering since it allows for the analytic integration of the kernel cross section over the scattering angle also for t and s-t contributions. Actually, the terms including $\alpha(t)$ involve the following kinds of integrands: α/t, $\alpha(t)$, $\alpha(t)t$, $\alpha(t)\chi(t)/t$, $\alpha(t)\chi(t)$, $\alpha(t)\chi(t)t$, $\alpha^2(t)/t^2$, $\alpha^2(t)/t$, $\alpha^2(t)$, where $\chi(t)$ stands for $(t-M_Z^2)^{-1}$. The analytic integration is much more lengthy then in the pure s case and it has been performed by using SCHOONSCHIP [27]. The result for the $F \pm B$ cross section can be written down in terms of elementary functions, logarithms, and Spence functions as shown in details in Appendix B. This is of some relevance because again numerical accuracy is guaranteed, and moreover the evaluation of large-angle Bhabha cross section is essentially on the same ground as the evaluation of a pure s-channel cross section, the slightly larger CPU time required being due only to the more complex form of the integrand and not to higher dimensionality integrals as in [14].

A last comment on the final-state QED correction is in order for Bhabha scattering. As already discussed in a previous section, different recipes in treating higher-order effects can lead to results differing by some per mills in the tails below and above the resonance, the uncertainty arising from this effect dominating the uncertainties due to the other approximations assumed. In the case of Bhabha scattering due to the presence of t-channel contributions this effect has been shown to be more marked [1] and therefore should be carefully taken into account when comparing different approaches.

The above formulation for the computation of QED

corrections to large-angle Bhabha scattering is implemented in the FORTRAN code TOPAZ0. Comparisons for the full Bhabha cross section and asymmetry between TOPAZ0, ALIBABA, and the Bhabha package of ZFITTER (BHANG) can be found in [1]. These comparisons show a very good agreement with ALIBABA, a slightly less satisfactory one with BHANG (see [1] for the interpretation of the discrepancies), but point out that the theoretical uncertainty in the computation of Bhabha observables is at least one order smaller than the present experimental error.

VIII. CONCLUSIONS

In this paper we have shown how to handle with the problem of including realistic experimental cuts within a SF approach to e^+e^- collisions around the Z^0 peak. The effect of cuts on the energies or invariant mass, scattering angles, and maximum acollinearity of the outgoing fermions has been included in the treatment of QED radiative corrections both for the initial- and final-state radiation. Based on a realistic description of the kinematics of the scattering process in the laboratory frame, analytical formulas for the boundaries of the allowed portion of the initial-state radiation phase space have been derived, thus allowing a semianalytical treatment of the corrected observables in the framework of the electron structure functions. Also, for the final-state QED corrections realistic cuts can be kept under control by means of completely analytic formulas with particular care to the inclusion of higher-order effects. Both s-channel annihilation and large-angle Bhabha scattering can be described by virtue of the general features of the formalism. Contrary to some recent statements in the literature [16], the SF approach can be employed to obtain accurate results for many realistic distributions of high-energy processes.

The actual motivation for this work was, as already stated in the Introduction, to build the tools necessary to carry out the program of directly analyzing LEP cross section and asymmetry data to extract information on the unknown parameters of the MSM. The above formulation for QED corrections at LEP and/or SLC energies, properly interfaced with a library for weak [6, 7], QCD [20], and heavy-top corrections [21], is implemented in the FORTRAN code TOPAZ0 [2], which is a program designed for computing observables and fitting cross sections and forward-backward asymmetries around the Z^0 peak, both for extrapolated and exclusive setup. Several physical results, comparisons with independent formulations, and limits on the unknown parameters of the MSM from various fits to LEP data as obtained by TOPAZ0 can be found in Ref. [1].

ACKNOWLEDGMENTS

We would like to thank Giampiero Passarino for having provided us with the FORTRAN codes for the molding of α and very helpful collaboration and discussions. INFN, Sezione di Pavia, is acknowledged for allowing the use of computer resources.

APPENDIX A: GENERAL FORMULA FOR CALORIMETRIC MEASUREMENT

We list here the formula for the hard collinear photon correction derived in the first paper of Ref. [18]:

$$\begin{aligned} C = &-\ln\varepsilon\left[\ln\left[1+\varrho^2(1-\varepsilon)^2\right]-\frac{\varrho^2}{1+\varrho^2}\right] \\ &+\left[\frac{(1+\varrho^2)^2-2}{4\varrho^2(1+\varrho^2)}-\left(1-\frac{1}{2}\varepsilon\right)^2\right] \\ &\times\ln\left[1+\varrho^2(1-\varepsilon)^2\right]-\frac{1}{\varrho}\frac{2+\varrho^2}{1+\varrho^2}\arctan\left[\varrho(1-\varepsilon)\right] \\ &+\frac{9}{4}-\frac{5}{2}\varepsilon+\frac{1}{4}\varepsilon^2+2\,\mathrm{Re}\left[f(\rho,\varepsilon)\right], \end{aligned} \tag{A1}$$

where $f(\varrho,\varepsilon)$ is defined as

$$\begin{aligned} f(\varrho,\varepsilon) = &-\ln(1+z)\ln\left(\frac{z}{1-\varepsilon+z}\right)+\mathrm{Li}_2\left(\frac{z}{1+z}\right) \\ &-\mathrm{Li}_2\left(\frac{1-\varepsilon+z}{1+z}\right) \end{aligned}$$

and z, ϱ, and ε are given by

$$z=\frac{i}{\varrho},\quad \varrho=\frac{\delta E}{m},\quad \varepsilon=\frac{\omega_0}{E}=1-\frac{E_0}{E}.$$

E_0 is the value of the calorimetric threshold, E the energy of the emitting leg. It is worth stressing that Eq. (A1) holds for any value of ϱ (compatible with $\delta \ll 1$) and ε, thus allowing for the evaluation of the hard collinear photon correction in the emission process by any lepton and without any limitation on the calorimetric threshold.

In the limit $\varepsilon \ll 1$ and for arbitrary ϱ, Eq. (A1) reduces to the photon spectrum given in the second and third paper of Ref. [18]. If $\varrho \gg 1$ is assumed, which holds true for electrons in the energy regime of LEP/SLC, almost independently of the value of δ, Eq. (A1) takes on the simpler form reported in Sec. IV.

APPENDIX B: INTEGRALS FOR BHABHA SCATTERING

In this appendix we report the relevant integrals which appear when integrating analytically the t-channel contributions of the Bhabha cross section over the angular acceptance with the molded formula for the running of $\alpha(t)$ as quoted in the text. We introduce the following notation: $\int_F dt$ stands for $\int_{t_0}^{t_{\max}} dt$, $\int_B dt$ stands for $\int_{t_{\min}}^{t_0} dt$, where $t_{\min} = -\frac{s}{2}(1+\cos\vartheta_{\min})$, $t_{\max} = -\frac{s}{2}(1-\cos\vartheta_{\min})$, $t_0 = -\frac{s}{2}$, and $dt = \frac{s}{2}d\cos\vartheta$. The $F \pm B$ contributions are obtained in a straightforward way by addition or subtraction:

$$\int_F dt\, \ln\left(\frac{-t}{\mu^2}\right) = t_0 - t_{\max} - t_0 \ln\left(\frac{-t_0}{\mu^2}\right) + t_{\max} \ln\left(\frac{-t_{\max}}{\mu^2}\right),$$

$$\int_B dt\, \ln\left(\frac{-t}{\mu^2}\right) = t_{\min} - t_0 - t_{\min} \ln\left(\frac{-t_{\min}}{\mu^2}\right) + t_0 \ln\left(\frac{-t_0}{\mu^2}\right),$$

$$\int_F dt\, t \ln\left(\frac{-t}{\mu^2}\right) = \frac{1}{4}\left[t_0^2 - t_{\max}^2 - 2t_0^2 \ln\left(\frac{-t_0}{\mu^2}\right) + 2t_{\max}^2 \ln\left(\frac{-t_{\max}}{\mu^2}\right)\right],$$

$$\int_B dt\, t \ln\left(\frac{-t}{\mu^2}\right) = \frac{1}{4}\left[t_{\min}^2 - t_0^2 - 2t_{\min}^2 \ln\left(\frac{-t_{\min}}{\mu^2}\right) + 2t_0^2 \ln\left(\frac{-t_0}{\mu^2}\right)\right],$$

$$\int_F dt\, \frac{1}{t} \ln\left(\frac{-t}{\mu^2}\right) = \frac{1}{2}\left[\ln^2\left(\frac{-t_{\max}}{\mu^2}\right) - \ln^2\left(\frac{-t_0}{\mu^2}\right)\right],$$

$$\int_B dt\, \frac{1}{t} \ln\left(\frac{-t}{\mu^2}\right) = \frac{1}{2}\left[\ln^2\left(\frac{-t_0}{\mu^2}\right) - \ln^2\left(\frac{-t_{\min}}{\mu^2}\right)\right],$$

$$\int_F dt\, \ln^2\left(\frac{-t}{\mu^2}\right) = -2t_0\left[1 - \ln\left(\frac{-t_0}{\mu^2}\right) + \frac{1}{2}\ln^2\left(\frac{-t_0}{\mu^2}\right)\right] + 2t_{\max}\left[1 - \ln\left(\frac{-t_{\max}}{\mu^2}\right) + \frac{1}{2}\ln^2\left(\frac{-t_{\max}}{\mu^2}\right)\right],$$

$$\int_B dt\, \ln^2\left(\frac{-t}{\mu^2}\right) = -2t_{\min}\left[1 - \ln\left(\frac{-t_{\min}}{\mu^2}\right) + \frac{1}{2}\ln^2\left(\frac{-t_{\min}}{\mu^2}\right)\right] + 2t_0\left[1 - \ln\left(\frac{-t_0}{\mu^2}\right) + \frac{1}{2}\ln^2\left(\frac{-t_0}{\mu^2}\right)\right],$$

$$\int_F dt\, \frac{1}{t^2} \ln\left(\frac{-t}{\mu^2}\right) = \frac{1}{t_0}\left[\ln\left(\frac{-t_0}{\mu^2}\right) + 1\right] - \frac{1}{t_{\max}}\left[\ln\left(\frac{-t_{\max}}{\mu^2}\right) + 1\right],$$

$$\int_B dt\, \frac{1}{t^2} \ln\left(\frac{-t}{\mu^2}\right) = \frac{1}{t_{\min}}\left[\ln\left(\frac{-t_{\min}}{\mu^2}\right) + 1\right] - \frac{1}{t_0}\left[\ln\left(\frac{-t_0}{\mu^2}\right) + 1\right],$$

$$\int_F dt\, \frac{1}{t^2} \ln^2\left(\frac{-t}{\mu^2}\right) = \frac{1}{t_0^2}\ln^2\left(\frac{-t_0}{\mu^2}\right) - \frac{1}{t_{\max}^2}\ln^2\left(\frac{-t_{\max}}{\mu^2}\right) + \frac{2}{t_0}\left[\ln\left(\frac{-t_0}{\mu^2}\right) + 1\right] - \frac{2}{t_{\max}}\left[\ln\left(\frac{-t_{\max}}{\mu^2}\right) + 1\right],$$

$$\int_B dt\, \frac{1}{t^2} \ln^2\left(\frac{-t}{\mu^2}\right) = \frac{1}{t_{\min}^2}\ln^2\left(\frac{-t_{\min}}{\mu^2}\right) - \frac{1}{t_0^2}\ln^2\left(\frac{-t_0}{\mu^2}\right) + \frac{2}{t_{\min}}\left[\ln\left(\frac{-t_{\min}}{\mu^2}\right) + 1\right] - \frac{2}{t_0}\left[\ln\left(\frac{-t_0}{\mu^2}\right) + 1\right],$$

$$\int_F dt\, \frac{1}{t} \ln^2\left(\frac{-t}{\mu^2}\right) = \frac{1}{3}\left[\ln^3\left(\frac{-t_{\max}}{\mu^2}\right) - \ln^3\left(\frac{-t_0}{\mu^2}\right)\right],$$

$$\int_B dt\, \frac{1}{t} \ln^2\left(\frac{-t}{\mu^2}\right) = \frac{1}{3}\left[\ln^3\left(\frac{-t_0}{\mu^2}\right) - \ln^3\left(\frac{-t_{\min}}{\mu^2}\right)\right],$$

$$\int_F dt\, \frac{1}{t - M_Z^2} = \ln\left(\frac{t_{\max} - M_Z^2}{t_0 - M_Z^2}\right),$$

$$\int_B dt\, \frac{1}{t - M_Z^2} = \ln\left(\frac{t_0 - M_Z^2}{t_{\min} - M_Z^2}\right),$$

$$\int_F dt\, \frac{\ln\left(\frac{-t}{\mu^2}\right)}{t - M_Z^2} = -\ln\left(\frac{-t_0}{\mu^2}\right)\ln\left(1 - \frac{t_0}{M_Z^2}\right) + \ln\left(\frac{-t_{\max}}{\mu^2}\right)\ln\left(1 - \frac{t_{\max}}{M_Z^2}\right)$$
$$+ \mathrm{Li}_2\left(\frac{-t_0}{M_Z^2 - t_0^2}\right) - \mathrm{Li}_2\left(\frac{-t_{\max}}{M_Z^2 - t_{\max}}\right) + \frac{1}{2}\ln^2\left(1 - \frac{t_0}{M_Z^2}\right) - \frac{1}{2}\ln^2\left(1 - \frac{t_{\max}}{M_Z^2}\right),$$

$$\int_B dt \frac{\ln\left(\frac{-t}{\mu^2}\right)}{t-M_Z^2} = -\ln\left(\frac{-t_{\min}}{\mu^2}\right)\ln\left(1-\frac{t_{\min}}{M_Z^2}\right)+\ln\left(\frac{-t_0}{\mu^2}\right)\ln\left(1-\frac{t_0}{M_Z^2}\right)$$
$$+\mathrm{Li}_2\left(\frac{-t_{\min}}{M_Z^2-t_{\min}^2}\right)-\mathrm{Li}_2\left(\frac{-t_0}{M_Z^2-t_0}\right)+\frac{1}{2}\ln^2\left(1-\frac{t_{\min}}{M_Z^2}\right)-\frac{1}{2}\ln^2\left(1-\frac{t_0}{M_Z^2}\right),$$

$$\int_F dt \frac{1}{(t-M_Z^2)^2} = \frac{1}{t_0-M_Z^2}-\frac{1}{t_{\max}-M_Z^2},$$

$$\int_B dt \frac{1}{(t-M_Z^2)^2} = \frac{1}{t_{\min}-M_Z^2}-\frac{1}{t_0-M_Z^2}.$$

[1] G. Montagna, O. Nicrosini, G. Passarino, F. Piccinini, and R. Pittau, Nucl. Phys. B (to be published) and references therein.

[2] G. Montagna, O. Nicrosini, G. Passarino, F. Piccinini, and R. Pittau, Comput. Phys. Commun. (to be published).

[3] G. Montagna, O. Nicrosini, and G. Passarino, Phys. Lett. B **303**, 170 (1993).

[4] E. A. Kuraev and V. S. Fadin, Yad. Fiz. **41**, 733 (1985) [Sov. J. Nucl. Phys. **41**, 466 (1985)]; G. Altarelli and G. Martinelli, in *Physics at LEP*, LEP Jamboree, Geneva, Switzerland, 1985, edited by J. Ellis and R. Peccei (CERN Report No. 86-02, Geneva, 1986); see also F. A. Berends *et al.*, in *Z Physics at LEP 1*, Proceedings of the Workshop, Geneva, Switzerland, 1989, edited by G. Altarelli, R. Kleiss, and C. Verzegnassi (CERN Yellow Report No. 89-08, Geneva, 1989), Vol. 1, p. 89, and references therein.

[5] O. Nicrosini and L. Trentadue, Phys. Lett. B **196**, 551 (1987); Z. Phys. C **39**, 479 (1988). For a review see also O. Nicrosini and L. Trentadue, in *Radiative Corrections for e^+e^- Collisions*, edited by J. H. Kühn (Springer, Berlin, 1989), p. 25; in *QED Structure Functions (Ann Arbor, MI, 1989)*, edited by G. Bonvicini, AIP Conf. Proc. No. 201 (AIP, New York, 1990), p. 12; O. Nicrosini, *ibid.*, p. 73.

[6] G. Passarino and M. Veltman, Nucl. Phys. **B160**, 151 (1979); G. Passarino, in *Radiative Corrections for e^+e^- Collisions* [5], p. 179; in *QED Structure Functions* [5], p. 132; G. Passarino and R. Pittau, Phys. Lett. B **228**, 89 (1989); G. Passarino and M. Veltman, *ibid.* **237**, 537 (1990); G. Passarino, in *Proceedings of the Joint International Lepton-Photon Symposium and Europhysics Conference on High Energy Physics*, Geneva, Switzerland, 1991, edited by S. Hegarty, K. Potter, and E. Quercigh (World Scientific, Singapore, 1992), Vol. 1, p. 56.

[7] G. Passarino, "QFORMFS, a computer program for the calculation of one loop scalar form factors" (unpublished); see also [2].

[8] M. Cacciari, G. Montagna, O. Nicrosini, and G. Passarino, Phys. Lett. B **279**, 384 (1992); M. Cacciari, G. Montagna, O. Nicrosini, G. Passarino, and R. Pittau, *ibid.* **286**, 387 (1992).

[9] M. Cacciari, A. Deandrea, G. Montagna, O. Nicrosini, and L. Trentadue, Phys. Lett. B **268**, 441 (1991); **271**, 431 (1991), and references therein.

[10] F. Piccinini and R. Pittau, Phys. Lett. B **293**, 237 (1992).

[11] G. Montagna, O. Nicrosini, and G. Passarino, Phys. Lett. B (to be published).

[12] W. Beenakker, F. A. Berends, and S. C. van der Mark, Nucl. Phys. **B349**, 323 (1991).

[13] S. Jadach, E. Richter-Was, B. F. L. Ward, and Z. Was, Phys. Lett. B **253**, 469 (1991); **260**, 438 (1991); S. Jadach and B. F. L. Ward, Phys. Rev. D **40**, 3582 (1989).

[14] D. Bardin *et al.*, Report No. CERN-TH.6433/92 (unpublished), and references therein; T. Riemann, in *Proceedings of the XXVIth International Conference on High Energy Physics*, Dallas, Texas, 1992, edited by J. Sanford, AIP Conf. Proc. No. 272 (AIP, New York, 1993); DESY Report No. DESY 91-144, 1992 (unpublished).

[15] M. Caffo, H. Czyz, and E. Remiddi, Nuovo Cimento A **105**, 277 (1992); "BHAGEN: an event generator of Bhabha scattering at Z energy, for small and large scattering angles" (unpublished).

[16] H. D. Dahmen, P. Manakos, T. Mannel, and T. Ohl, Z. Phys. C **50**, 75 (1991).

[17] D. Levinthal, F. Bird, R. G. Stuart, and B. W. Lynn, Z. Phys. C **53**, 617 (1992).

[18] M. Cacciari, G. Montagna, and O. Nicrosini, Phys. Lett. B **274**, 473 (1992). See also M. Caffo, R. Gatto, and E. Remiddi, Phys. Lett. **139B**, 439 (1984); Nucl. Phys. **B252**, 378 (1985); G. Sterman and S. Weinberg, Phys. Rev. Lett. **39**, 1436 (1977); J. Fleisher and F. Jegerlehner, Z. Phys. C **26**, 629 (1985); M. Greco, Riv. Nuovo Cimento **11**, 1 (1988).

[19] M. Caffo, E. Remiddi, and F. Semeria, in *Z Physics at LEP 1* [4], p. 171, and references therein.

[20] A. L. Kataev, Report No. CERN-TH.6465/92, 1992 (unpublished); K. G. Chetyrkin, J. H. Kühn, and A. Kwiatkowsky, Phys. Lett. B **282**, 221 (1992); K. G. Chetyrkin and J. H. Kühn, *ibid.* **248**, 359 (1990).

[21] R. Barbieri, M. Beccaria, P. Ciafaloni, G. Curci, and A. Viceré, Report No. CERN-TH.6713/92 (unpublished); Phys. Lett. B **288**, 95 (1992). See also [14] and references therein.

[22] B. A. Kniehl, M. Krawczyk, J. H. Kühn, and R. G. Stuart, Phys. Lett. B **209**, 337 (1988); S. Jadach, M. Skrzypek, and M. Martinez, *ibid.* **280**, 129 (1992).

[23] G. Montagna, O. Nicrosini, and L. Trentadue, Phys. Lett. B **231**, 492 (1990); see also M. Böhm *et al.*, in *Z Physics at LEP 1* [4], Vol. 1, p. 203, and references therein.

[24] T. Kinoshita, J. Math. Phys. **3**, 650 (1962); T. D. Lee and M. Nauenberg, Phys. Rev. **133**, B1549 (1964); J. Collins, D. Soper, and G. Sterman, in *Perturbative QCD*, edited by A. H. Mueller (World Scientific, Singapore, 1989), and references therein.

[25] H. Burkhardt, F. Jegerlehner, G. Penso, and C. Verzegnassi, Z. Phys. C **43**, 497 (1989).

[26] See [9, 12–17, 19] and references therein; see also F. Aversa and M. Greco, Phys. Lett. B **271**, 435 (1991); F. Aversa, M. Greco, G. Montagna, and O. Nicrosini, *ibid.* **247**, 93 (1990); M. Böhm, A. Denner, and W. Hollik, Nucl. Phys. **B304**, 687 (1988); F. A. Berends, W. Hollik, and R. Kleiss, *ibid.* **B304**, 712 (1988); F. A. Berends and R. Kleiss, *ibid.* **B228**, 737 (1983).

[27] M. Veltman, SCHOONSCHIP, a program for symbol handling" (unpublished); see H. Strubbe, Comput. Phys. Commun. **8**, 1 (1974).